J. nat. Rubb. Res., **6(4)**, 267-280

Drying of Natural Rubber in Sheet Form – Internal Structure and Water Transfer

R. AURIA*, J.C. BENET**, B. COUSIN** AND J. SAINTE-BEUVE***

The internal structure of hydrated natural rubber was revealed by observation under the electron scanning microscope, using the cryofracturing technique. It showed that natural rubber in its hydrated state is made up of an agglomeration of rubber globules which retain their original shape and size and it is a diphasic medium during drying. The internal water transfer in a sheet of natural rubber during the falling rate drying period was studied. Experimental analysis of the development of water content profiles in the sheet substantiated a law of water transfer using the water content gradient as the thermodynamic transfer force. The coefficient of transfer involved in the law was measured, and proved to be highly dependent on the water content.

Research work on plant physiology has produced quite a detailed picture of latex rubber in liquid form. The rubber globules are spherical, ovoid or pyriform in shape. Dimensions[1] vary between 0.02 μm and 6 μm. There has been little work on the internal structure of rubber after coagulation. The only description of this structure was given by Southorn[2] who revealed pockets of moisture trapped in the mass, measuring about 1 μm. This description of the internal structure of rubber is, however, incomplete: in particular, it is not known whether during drying, the structure comprises an agglomeration of globules whose original characteristics remain intact (dimension, shape, composition), or if latex coagulation and the milling operation and drying of the coagulum are accompanied by significant changes in the globules. Furthermore, it is not known whether during drying, natural rubber can be likened to a diphasic medium (rubber globules + serum), or whether there is also a gaseous phase, making it triphasic.

There is little literature on drying natural rubber sheets. Preliminary work[3,4] identified the various drying periods: a period at constant speed, followed by a period at decreasing speed. The latter itself breaks down into two phases: the first known as 'intermediate' or 'non-saturated surface' and the second 'diffusive'.

During the first drying period, it is taken that the internal mechanisms drawing humidity from inside the products are sufficiently rapid to keep the surface saturated in serum[4,5]. Drying speed then depends on the aerothermal qualities of the air used for drying. Heating the film of water on the surface balances the energy required for vaporisation. Drying is isenthalpic and temperature of the sheet equal to the temperature indicated on the wet bulb thermometer[5,6]. The transfer of heat at the interface, through the outer layer, governs the drying process.

After the first drying period, there is an 'intermediate' phase characterised by a rapid

*ORSTOM (Institut Francais de Recherche Scientifique pour le Développement en Coopération), 213 rue Lafayette, 75480 Paris Cedex 10, France

**Laboratoire de Mécanique Générale des Milieux Continus, URA CNRS 1214, Universite de Montpellier II, Place E. Bataillon, 34095 Montpellier Cedex, France

***IRCA/CIRAD (Institut de Recherches sur le Caoutchouc), 42 rue Scheffer, 75116 Paris, France

decrease in drying speed. This decrease is linked to a reduction in the fraction of the sheet's surface which is completely saturated. Researchers[3-6] agree that the end of this first period corresponds to a water content of 10%.

One the water content is less than 10%, the drying speed decreases considerably. This new 'diffusive' phase accounts for more than 90% of the total drying time. Initial research into this phase led to an experimental linear relationship between drying time and the square of the thickness of the sheets. The relationship corresponds to a Fickian-type[4] theoretical approach; it is also suggested that internal water transport regulates drying mechanisms and is the diffusive type. Nonetheless, certain authors[6,7] claim that the coefficient of diffusion varies according to the water content.

The studies mentioned above approach the problem of drying of natural rubber from an overall point of view, based on the analysis of drying kinetics. The empirical formulae proposed are of limited validity and the results are not very precise. These approaches mask the contributions made by various internal humidity transport mechanisms which occur during the drying of rubber sheets. They also do not take into account the 'crust' which appears on the suface of the sheet at the beginning of the diffusive drying phase. This phenomenon plays a predominant role in the process of drying kinetics.

Contributions are made in the following areas:

- Observation of internal structure in the hydrated state
- Elaboration of a mathematical model for water transport during the period of decreased drying speed
- Experimental study of the internal water transport mechanism during the period of decreased drying speed, measurement of the coefficient of water transport and study of its variation depending on the water content.

MICROSCOPIC OBSERVATIONS OF RUBBER IN THE DEHYDRATED AND HYDRATED STATES

Materials and Methods

The latex used for these experiments came from IRCA in Cote d'Ivoire and dry rubber content (d.r.c.) was 37%. To prevent spontaneous coagulation of rubber particles, the latex was stabilised using a diluted ammonia solution (9 g/litre of latex). After dilution to a reference d.r.c. of 15%, coagulation of the rubber particles was carried out by adding diluted acetic acid (5%). To characterise the intensity of milling, the machining ratio (M.R.), calculated by dividing the gap between the rollers by the average thickness of the coagulum, was 0.15.

For observations in the dehydrated state, the samples were taken from a sheet of natural rubber which had been completely dehydrated in an oven at a constant temperature of 50°C.

For observations in the hydrated state, the thickness of the hydrated natural rubber sheet was 4 mm. This sheet was dried in an oven for 10 h at 50°C. Samples with a mean water content of about 13% were taken from the centre of the sheet; the samples were rods of about 0.5×2 mm. The cryofracturing technique was used to prepare the samples for observation, and consists of creating a fracture in the pre-frozen sample. The sample was placed in two half-cups with an internal diameter of 1 mm frozen in liquid nitrogen (–150°C), then placed in a high vacuum (2×10^{-6} to 3×10^{-6} mm Hg). The sample was fractured by a tractive force on the two half-cups. The fracture surface was cleaned by sublimating the ice, by raising the temperature to about –50°C. A very fine carbon-platinum coating was applied to the structural details uncovered by cleaning; this means that a replica of the cryofractured surface can be obtained, suitable for observation under the electron microscope. The main advantage of the cryofracturing technique is that it prevents the formation of artefacts, as would be the case when using a chemical agent to fix water.

Results

Figure 1 shows the surface of the sample observed under an electron microscope. This is the most characteristic state of the surface of dehydrated natural rubber. No significant porosity can be seen, and this structural compactness was checked on several samples. 'Nodules' of about 20–30μm in size on the average (the whiter areas in the photo) can also be seen. The origin of these 'nodules' is not fully known, but they may consist of agglomerated globules which were not amalgamated into the mass during coagulation.

Figures 2 and *3*, taken from different angles and enlarged to different degrees, show the internal structure of hydrated natural rubber. They suggest that this structure is composed of agglomerated latex particles. Despite coagulation, milling and drying, it would appear that, overall, these particles preserve their original shape. Taken together, these globules seem to constitute a relatively tight network, which in turn creates a number of loosely connected cavities.

DOES NATURAL RUBBER HAVE A DIPHASIC OR TRIPHASIC STRUCTURE DURING DRYING?

It is proposed to study whether the inter-globular space detected (*Figures 2* and *3*) is entirely occupied by a liquid phase, constituted by the serum, or if, at the temperature of 50°C commonly used for drying sheet, a gaseous phase (air + steam) is produced. The method used consists of comparing variations in the apparent mass density of the product as a function of the

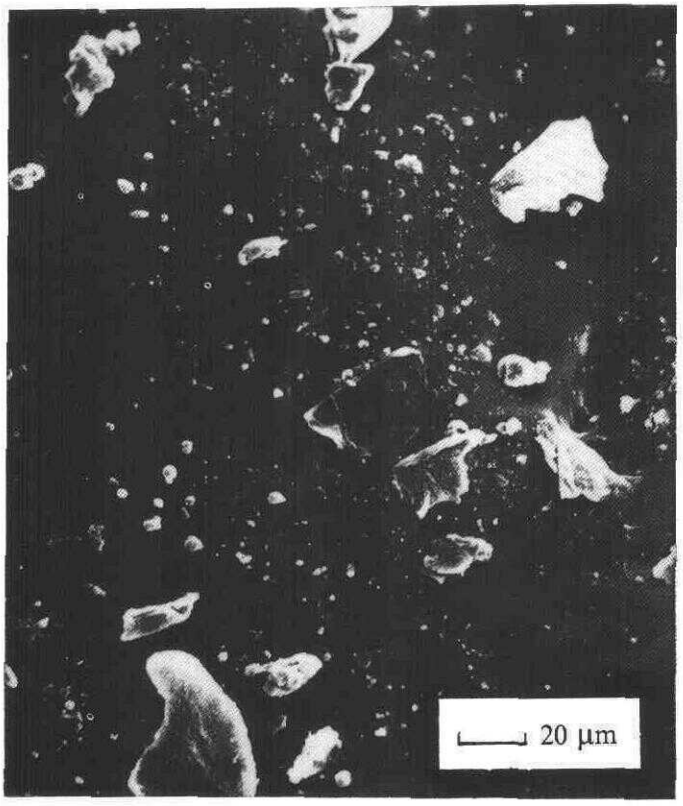

Figure 1. Surface of dehydrated natural rubber sheet.

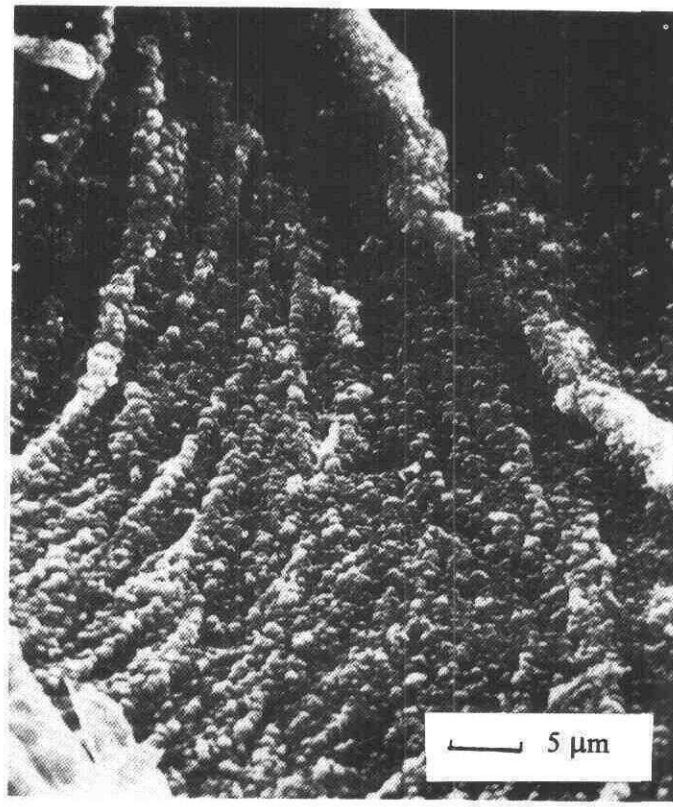

Figure 2. Internal structure of hydrated natural rubber (w = 13%).

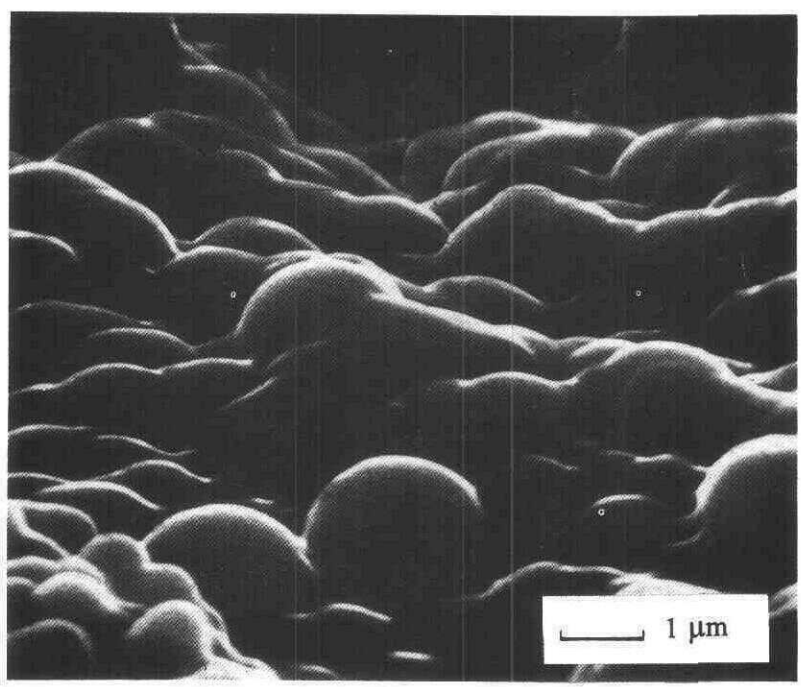

Figure 3. Internal structure of hydrated natural rubber from an acute angle.

water content, obtained experimentally, with an analytical relationship between the two variables, based on the hypothesis of a diphasic structure. The comparison will enable the validity of the hypothesis to be judged.

STRUCTURAL CONTRACTION

Materials and Methods

Natural rubber samples with an initial water content of 35% and thicknesses of between 0.8 mm and 4 mm are placed in a drying chamber. The air in the unit is kept at 50% relative humidity using sulphuric acid solution; the temperature is kept at 50°C by a thermostatically-controlled bath[8]. At various points in the drying cycle, samples are taken; mass of water m_e and volume V are measured in the hydrated state and mass of the sample m_s in the anhydrous state. Volume V is measured by determining the volume displaced when the sample is immersed in mercury, and mass m_s using an accurate weighing scale (0.1 mg), after complete desiccation. The mean water content $w = m_e/m_s$ and the apparent mass density $\rho_s = m_s/V$ are deduced from this.

Results

The points in *Figure 4* represent the variation in the apparent mass density of the solid phase of rubber ρ_s, depending on the mean water content w of the sample, within a water content range of 0% to 32%. For an analytical interpretation of the experimental relationship revealed by *Figure 4*, assume that natural rubber has a diphasic structure. Under these conditions, the additivity of the volumes of rubber and water makes it possible to express the apparent mass density ρ_s, depending on the mean water content w, by:

$$\rho_s = \rho^*_s \rho^*_e / (\rho^*_e + \rho^*_s w) \quad \ldots 1$$

where ρ^*_s : true mass density of water (0.99 g/cm³)

ρ^*_s : true mass density of the solid phase of natural rubber.

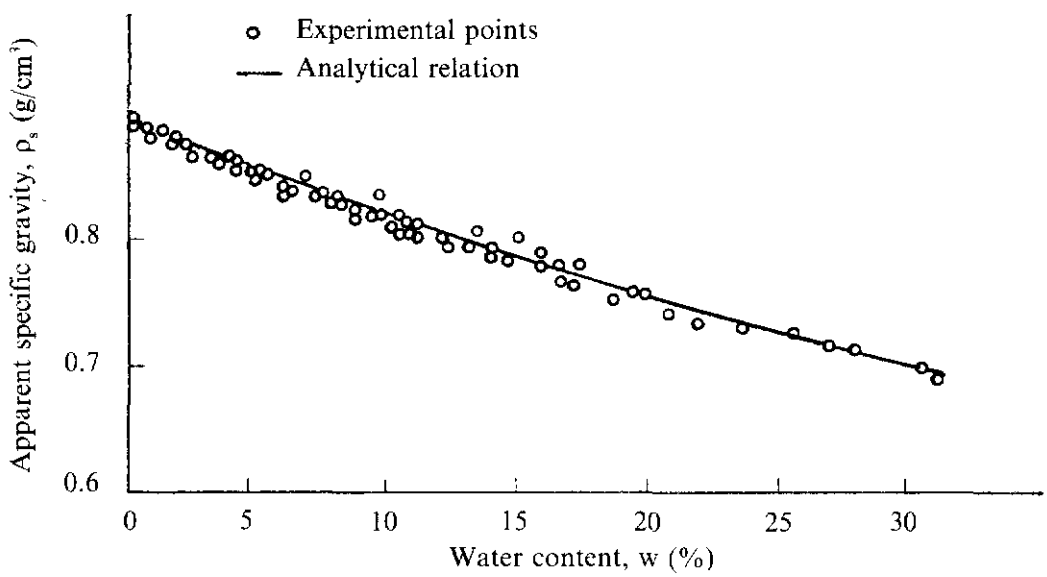

Figure 4. Variation in the apparent specific gravity of natural rubber depending on water content.

The electron micrograph showed *(Figure 1)* that natural rubber in its dehydrated state, is compact; the real mass density of the solid phase of natural rubber ρ^*_s is assumed to be independent of the water content and equal to the apparent mass density value ρ_s for nil water content. According to *Figure 4*, this value is equal to 0.893 g/cm^3. *Equation 1*, represented in *Figure 4* as a continuous line, is a good approximation of the experimental figures as a whole. The close agreement between the experimental figures and the theory suggests that the diphasic hypothesis, on which *Equation 1* is based, is satisfactory.

MODEL FOR ISOTHERMAL WATER TRANSPORT DURING THE DIFFUSIVE PHASE

Once the diphasic structure hypothesis is adopted, it is possible to assimilate the liquid phase to pure water. In addition, it is taken that temperature of the sheet is uniform and constant during the period of decreasing speed; this hypothesis will be checked experimentally. The water content (w) is chosen as a variable of state.

Water mass balance equation

The water mass balance in a heterogenous medium[9] is expressed by:

$$\frac{\partial}{\partial t}\rho_e = -\operatorname{div}(\rho_e V_e)$$

where ρ_e : apparent mass density of liquid water

V_e : phenomenological speed of liquid water

Taking water content $w = \rho_e / \rho_s$ as a ariable, the water mass balance can be expressed as follows:

$$\frac{\partial}{\partial t}(\rho_s w) = -\operatorname{div}(\rho_e V_e) \qquad \ldots 2$$

Phenomenological transport relationship

Without taking gravity into account, the application of irreversible linear process thermodynamic methods leads to the adoption of phenomenological water transport relationship/ratio of the following type[8,10]:

$$\rho_e V_e = -D.\ \text{grad}\ \mu_e \qquad \ldots 3$$

where μ_e is the molar chemical potential of liquid water and D is the thermodynamic diffusion coefficient of water in natural rubber[10].

Equations of state

To exploit *Equations 2* and *3*, it is necessary to express the variables μ_e and ρ_s by two equations of state as a function of the variable of state w. In an isothermal process, the water's chemical potential μ_e is equal to the molar chemical potential of water vapour in equilibrium μ_{ve}:

$$\mu_e = \mu_{ve} = RT \ln \frac{P_v}{P_{vs}} \qquad \ldots 4$$

where R = the constant of ideal gases, T = air temperature, P_v = partial pressure of water vapour in equilibrium, P_{vs} = saturated vapour pressure at temperature T.

The desorption isotherm provides a relationship between P_v and w

$$P_v = h(w) \qquad \ldots 5$$

However, for natural rubber, current measuring techniques do not enable the partial pressure of equilibrium P_v to be accurately determined when water content exceeds about 2%, though *Equation 5* exists whatever the water content.

Combining *Equations 4* and *5*,

$$\mu_e = RT \ln [h(w)] = f(w) \qquad \ldots 6$$

The relationship between ρ_s and w which indicated structural contraction is given by *Equation 1*. Within the water content interval studied ($w < 20\%$), *Equation 1* can be approximated using a linear relationship of the type:

$$\rho_s = \rho^*_s - \rho^{*2}_s/\rho^*_e \quad \ldots 7$$

where ρ^*_e = true mass density of water

ρ^*_s = true mass density of the solid phase of natural rubber.

Model for the isothermal transport of water

Given *Equations 3* and *6*, the phenomenological relationship/ratio of water transport can be written as:

$$\rho_e V_e = -D.\,\mathrm{grad}\, f(w) = -D_1.\,\mathrm{grad}\, w \quad \ldots 8$$

$$\text{where } D_1 = D.\frac{\partial f}{\partial w} \quad \ldots 9$$

The mass balance *(Equation 2)* becomes:

$$\frac{\partial}{\partial t}(\rho_s . w) = \mathrm{div}\,(D_1.\,\mathrm{grad}\, w) \quad \ldots 10$$

Equation 10 completed by *Equation 7* forms a model for the isothermal transport of water within natural rubber.

WATER TRANSPORT MECHANISM DURING THE DIFFUSIVE PERIOD

Based on the phenomenological model of water transport described above, an experimental study was developed to analyse the internal mechanisms of water transport during the drying period at decreasing speed. The purpose of the study was to:

- validate the phenomenological relationship/ratio of water transport adopted *(Equation 8)*
- study variations in the coefficient of isothermal water transport D_1, depending on the water content.

Materials and Methods

The experiments consist of placing sheet rubber samples in a temperature and humidity regulated drying chamber *(Figure 5)* and monitoring, over time, the changes in the water content and temperature profiles of these samples in the direction of transfer, *i.e.* perpendicular to the surfaces of the sheet.

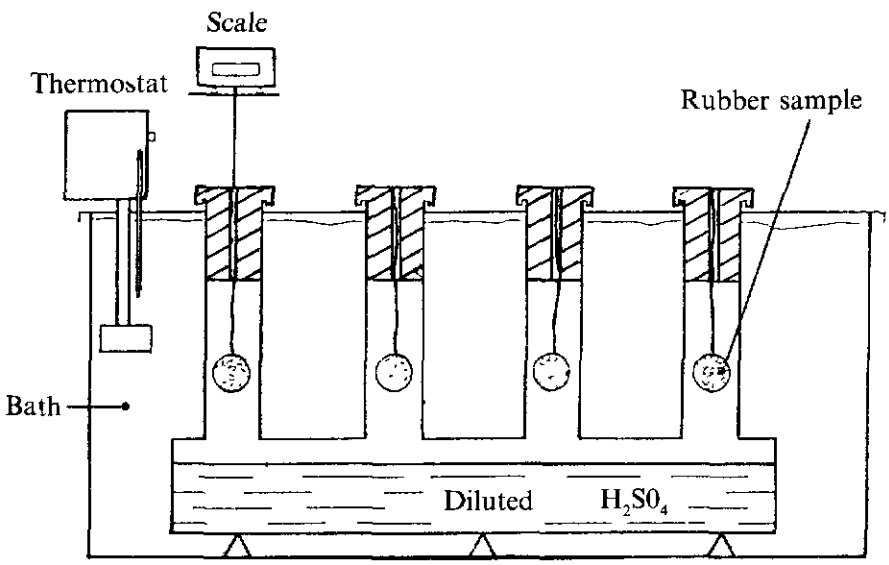

Figure 5. Experimental design.

A solution of diluted sulphuric acid keeps the relative humidity of the drying atmosphere at 50%. The temperature is regulated at 60°C.

After the milling operation, the rubber sheet is pressed slightly to give it a uniform thickness of 8 mm. Using a rotary borer, samples 25 mm in diameter are taken from the sheet and placed in the different tubes of the drying chamber. One of the samples is weighed continually. Thermocouples placed in another sample make it possible to monitor changes in the temperature profiles. The air temperature in the tubes is measured using thermocouples placed near the sample.

The other samples are intended for determining water content, by cutting off thin strips perpendicular to the direction of transfer. At different moments during drying, a sample is removed from the chamber for this purpose.

To minimise edge effects, a cylindrical sample, 14 mm in diameter is taken from the middle of the 25 mm sample; this new sample is weighed then enclosed in a silicon mould; to solidify the water profiles and facilitate cutting, the sample in the mould is frozen in liquid nitrogen. It is then cut into 0.6 mm thick strips using a circular saw. During the cutting operation, the mould-sample assembly is kept frozen by Peltier effect elements. The water content in each strip is measured by weighing them in their hydrated and anhydrous states. Within the water content interval studied ($w < 20\%$), it was shown that the techniques used (freezing, cutting) do not cause water loss or profile disruption and that the profiles determined on the different samples are representative of the evolution in a single sample[8].

Results

Figure 6 shows the evolution of the water content profile obtained on the half-

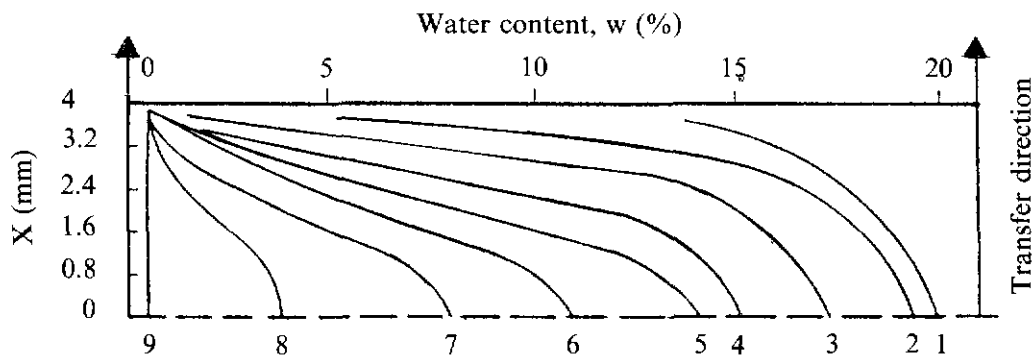

No.	Time (h)	Mean water content (%)
1	0	17.8
2	18	15.2
3	42	12.6
4	74	10.0
5	114	6.0
7	258	3.9
8	430	1.9
9	795	0.5

Figure 6. Evolution of the water content profile.

thickness of the sample. These profiles were established after checking the symmetry of experimental points compared to the median plane of the sheet.

All these profiles reveal steep water content gradients that can reach 100/m in certain areas of the sheet. After 42 h of drying *(Profile 3)*, it can be seen that the water profile equilibrium is reached on the surface. This value (w = 0.5%) corresponds to the mean water content equilibrium reached by the sample at the end of drying *(Profile 9)*. This result tallies with the water content value obtained from desorption isotherms at 60°C[5,8]. It should be noted that product equilibrium on the surface is characterised by the appearance of a thin brownish layer, which marks the appearance of the 'crusting' phenomenon. The appearance of a point of inflection can be seen near the surface on profiles with a water content of 6%, 7% and 8%. A zone where water contents are practically nil (crusting zone) spreads towards the centre of the sheet during drying *(Profiles 7* and *8)*.

The evolution of the temperature profile depending on thickness is shown in *Figure 7*. Temperature distribution in the sample is virtually uniform, with a mean value of 59.5°C throughout the experiment. The thermocouple placed near the sample in the drying atmosphere shows that the difference between the air temperature and the mean temperature of the sample does not exceed 1°C. It can be concluded that no appreciable thermal imbalances exist between the sample and the atmosphere. The temperature measurements support the hypothesis that the isothermal drying method used in this study was well adapted.

Validation of the phenomenological relationship/ratio of water transport. In the experiments conducted, transfers can be considered as unidirectional depending on the thickness of the sheet (direction X in

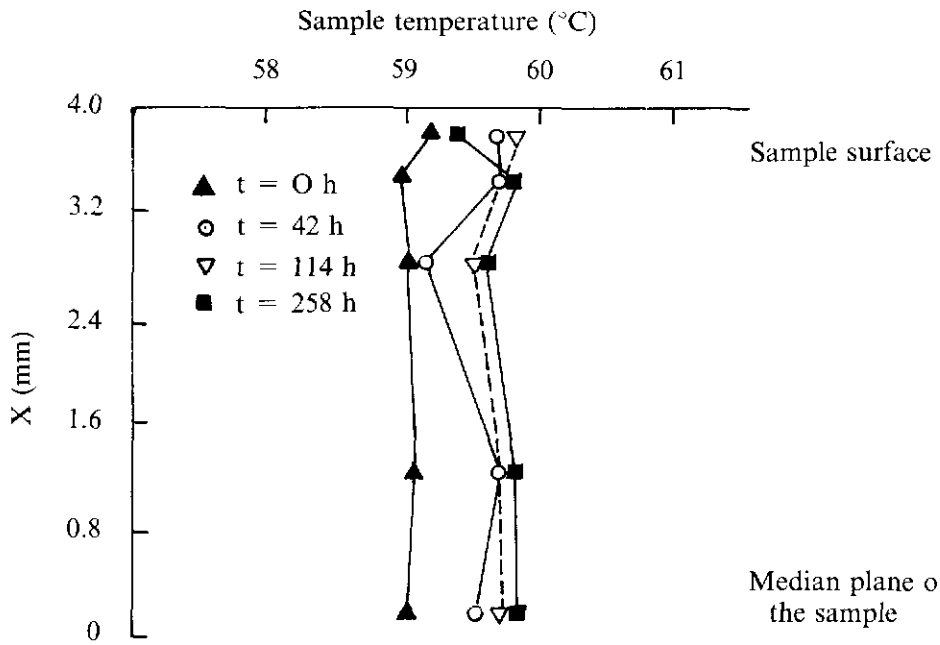

Figure 7 Evolution of the temperature profile.

Figure 6). Depending on this direction, *Equation 8* is written:

$$\rho_e V_{ex} = - D_1 \frac{\partial w}{\partial x} \quad \ldots 11$$

where $\rho_e V_{ex}$ is the flow density in direction X.

To check this relationship/ratio, it is necessary to determine the thermodynamic force $\partial w/\partial x$ and evaluate water transport flow density $\rho_e V_{ex}$ depending on the direction X; the water content gradient is deduced directly from the profiles in *Figure 6*. Determination of flow density $\rho_e V_{ex}$ is carried out using the mass balance *Equation 2*; by carrying over *Relationship 7* into *Relationship/ratio 2*, this becomes:

$$\frac{\partial}{\partial t}(\alpha w^2 + w) = - \frac{1}{\rho^*_s} \frac{\partial (\rho_e V_e)}{\partial X} \quad \ldots 12$$

where $\alpha = - \rho^* s / \rho^* e$

By integrating *Relationship 12* between 0 to x and instant t, this becomes:

$$\rho_e V_{ex}(x,t) - \rho_e V_{ex}(0,t) = - \rho^*_s \frac{\partial}{\partial t} \int_0^x (\alpha w^2 + w)\, dx \quad \ldots 13$$

where V is the integration variable.

The hypothesis of symmetry compared to the median plane of the sheet entails nil flow for $X = O$ $\rho_e V_{ex}(0,t) = 0$. At a given point and instant, flow density is calculated by the relationship/ratio:

$$\rho_e V_{ex}(x.t) = - \frac{\partial}{\partial t} \rho_s \int_0^x (\alpha w^2 + w)\, dx \quad \ldots 14$$

Figures 8, 9 and *10* represent the variation in flow density $\rho_e V_{ex}$ depending on thermodynamic force $\partial w/\partial x$ for water content values of between 5% and 15%.

It can be seen that the linearity between flow and force is respected. These figures validate *Equation 11* in the water content range.

Variation in the coefficient of isothermal water transport depending on water content. Based on the profiles in *Figure 6*, and using the approach described above, it is possible to determine the value of the coefficient of isothermal water transport D_1 for different water content values within the range $2\% < w < 16\%$. *Figure 11* shows the variation in coefficient D_1 depending on water content w. It is seen that the coefficient depends very heavily on the water content; it reaches a minimum for a water content w of about 10%.

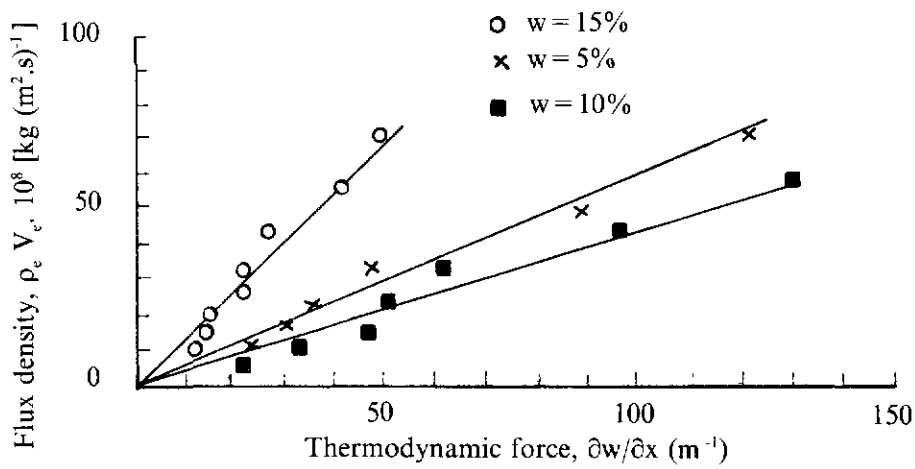

Figure 8. Variations in water flow density depending on the water content gradient, w = 5%, 10%, 15%.

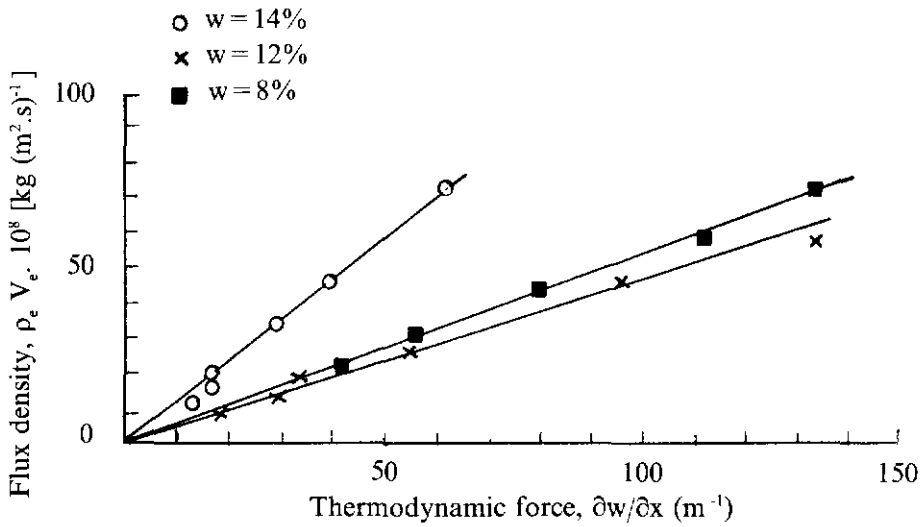

Figure 9. Variations in water flow density depending on the water content gradient, w = 8%, 12%, 14%.

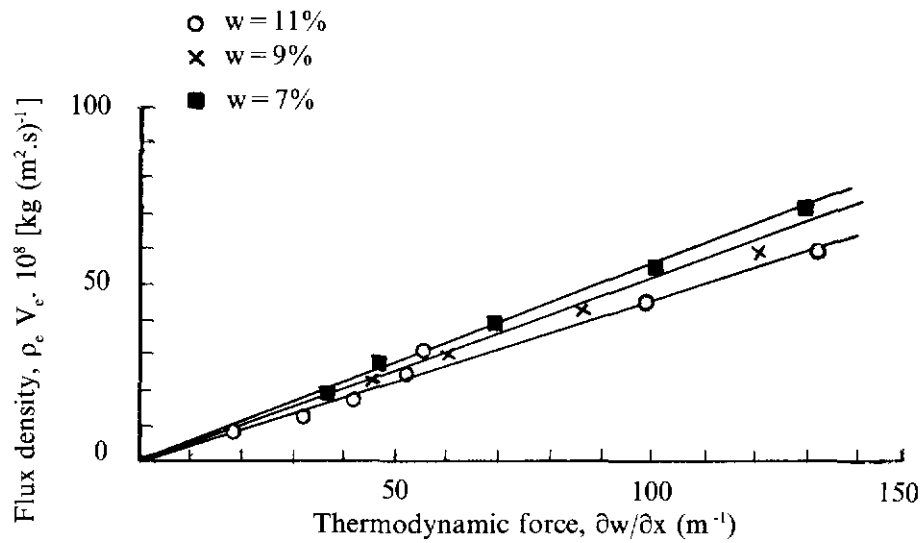

Figure 10. Variations in water flow density depending on the water content gradient, w = 7%, 9%, 11%.

This type of variation in the diffusive coefficient depending on water content has been observed by Budiman[6] during drying kinetics.

CONCLUSION

Preparing hydrated natural rubber samples using cryofracturing is well suited to

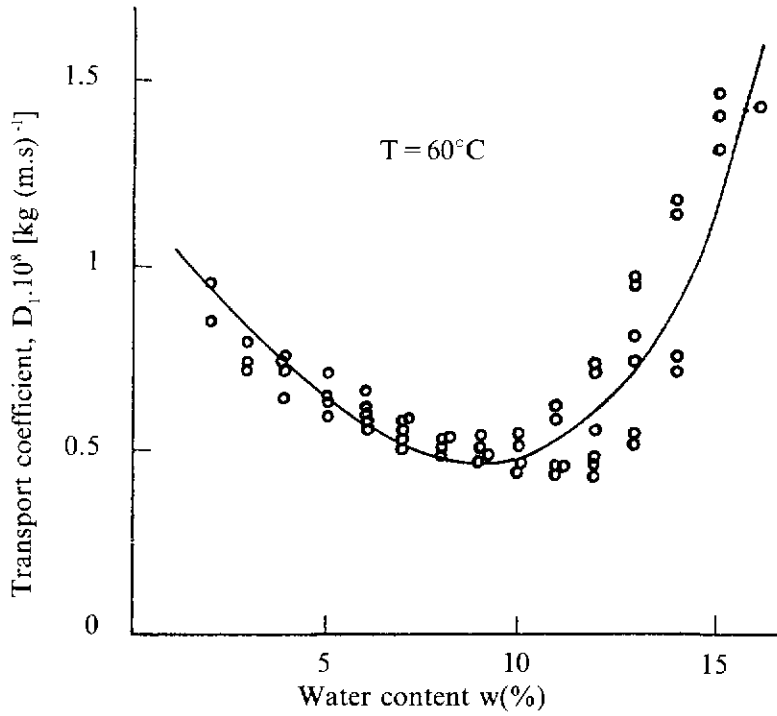

Figure 11. Variations in the water transport coefficient depending on water content.

observations of this type of material. The structure observed, consisting of interlinked rubber globules, seems to us to be characteristic of hydrated natural rubber. At a temperature of 50°C, it was shown that natural rubber remains a diphasic medium during drying: the space between the globules is entirely occupied by serum. According to a plan proposed by Vanderhoff *et al.*[11], the drying process apparently leads to the globules gradually coming together until a compact state is reached, corresponding to the dehydrated structure observed. The picture of the internal structure of hydrated natural rubber obtained during this study shows that modelling the drying process for this product can be steered towards diphasic models, with water transferred by filtration into the space between the globules.

Exact details of the links between the globules have not yet been established, but it seems, from the images obtained, that coagulation leads to a split in the phospholipoprotein layer around the globules[12], enabling links between the *cis* 1, 4 polyisoprene macromolecules which are the major constituents of rubber[1]. An understanding of the two phenomena which occur during drying – synaeresis, which, at high water contents, is seen in a spontaneous oozing of the serum, and hardening, which inhibits water transfer at low water contents – depends on our knowledge of links between globules and of the interaction between solid and liquid phases. Implementing the observation technique developed during this study of kinetics throughout the drying process should provide information on the structural modifications in rubber and steer drying models towards taking account of the interaction between distortions of the solid structure and water transfer.

On a theoretical level, adopting the chemical potential gradient as the thermo-

dynamic transfer force leads, once simplified, to a description of transfer phenomena using a FICK type law with a variable coefficient Expressing this coefficient brings the desorption isotherm gradient into play The standpoint adopted in this study, which attempts to establish a law of transfer based on a chemical potential gradient, is similar to that of Ghermann and Kast[13] The difficulty of using this approach in our case lies in the fact that it is impossible to accurately determine the desorption isotherm for water contents of more than 2%, since natural rubber is not a very hygroscopic material

On an experimental level, determining water content profiles in a sheet during drying revealed that the 'hardening' area progresses towards the centre of the sheet Exploitation of these profiles justifies, within the range of water contents investigated, the adoption of a law using the water content gradient as the mass transfer potential It has been shown that the coefficient of transfer reaches a minimum for the water content corresponding to the second critical point during drying This apparent variation is as yet unexplained, but observations currently under way on hydrated structure of natural rubber throughout the drying process should provide an explanation of the type of variation in the coefficient of transfer depending on the water content According to Vanderhoff *et al*[14], it is likely that by bringing them closer together, the interfacial forces between the particles are responsible for increasing the coefficient of diffusion at low water contents

ACKNOWLEDGEMENTS

This research programme was financed by the Institut Français de Recherche Scientifique pour le Developpement en Coopération (ORSTOM), GRECO CNRS 72 'Drying and transport mechanisms in non-saline porous media', the Conseil Regional du Languedoc Roussillon as part of the programme 'Agricultural and food product drying', the Institut de Recherches sur le Caoutchouc (IRCA), and the Mission Technologie Agricole et Alimentaire (CIRAD)

Date of receipt September 1990
Date of acceptance October 1991

REFERENCES

1 COMPAGNON P (1986) *Le caoutchouc naturel* collection Techniques agricoles et Productions Tropicales, Edition Maisonneuve et Larose, Paris

2 SOUTHORN, W A (1964) Electron Microscopy of Partially Dried Sheet Rubber *J Rubb Res Inst Malaya* **18(4),** 151

3 VAN HARPEN (1930) Un exemple de la production scientifique et economique de caoutchouc de plantation fume *Revue gen Caoutch* , 103

4 PIDDLESDEN J H (1937) The Drying of Rubber *J rubb Res Inst Malaya* **7,** 117

5 GALE, R S (1959) A Survey of Factors Involved in an Experimental Study of Sheet Rubber *J Rubb Res Inst Malaya* **16,** 38

6 BUDIMAN, S (1973) Water Removal from Natural Rubber Hydrogel Master of Science Thesis, Ohio State University

7 GALE, R S (1962) Drying of Sheet in the Falling Rate Period *Transactions,* **38,** 91

8 AURIA R (1988) Contribution a l'etude du caoutchouc naturel structure interne et transfert d humidite lors du sechage These de Doctorat, Universite des Sciences et des Techniques du Languedoc (USTL) Montpellier II

9 TRUESDELL, C AND TOLPIN, R (1960) The Classical Field Theories Handhoch der Physik Band III 1 Springer-Verlag, Berlin

10 PARK C S The Diffusion of Some Halo-methanes in Polystyrene *Trans Faraday Soc* , **46,** 684

11 VANDERHOFF J W BRADFORD, E B AND CARRINGTON W K (1973) The Transport of Water through Latex Films *J Polym Sci* **41,** 155

12 GOMEZ, J B AND SUBRAMANIAM A (1984) Some Recent Electron Microscopic Studies of *Hevea* Latex Particles *Proc nat Rubb Res Conf Kuala Lumpur* 510

13 GHERMANN, D AND KAST, W (1978) Drying of Gels *Proc First Int Symp Drying Montreal Canada (Mujumdar A S ed)*, 239 Science Press Princeton

14 VANDERHOFF, J W , TARKOWSKI, H L , JENKINS M C AND BRADFORD E B (1966) Theoretical Consideration of the Interfacial Forces Involved in the Coalescence of Latex Particles *J Macromol Chem* **1,** 361

APPENDIX

LIST OF SYMBOLS

$D.D_1$	Coefficients of isothermal water transport in a sheet of natural rubber
D.r.c.	Dry rubber content
M_e	Molecular weight of water
MR	Lamination rate
m	Total sheet weight
m_e	Weight of water in a sheet of natural rubber
m_3	Anhydrous sheet weight
P_v	Partial pressure of water vapour
P_{vs}	Pressure of saturating vapour
R	Constant of ideal gases
t	Time
T	Temperature
V_e	Phenomenological speed of liquid water
W	Water content
W_{c1}	Mean water content at the first critical drying point
W_{c2}	Mean water content at the second critical drying point
x	Co-ordinate on an axis perpendicular to the sides of the sheet

GREEK SYMBOLS

μ_e	Chemical potential of water
μ_{ve}	Chemical potential of water vapour in thermodynamic equilibrium with the water in rubber
ρ_e	Apparent specific gravity of water
ρ_s	Apparent specific gravity of the solid phase
ρ^*_e	True specific gravity of water
ρ^*_s	True specific gravity of natural rubber